**J. T. Katsikadelis**
Associate Professor of Structural Analysis,
Department of Civil Engineering,
National Technical University of Athens,
Athens, Greece 147

**L. F. Kallivokas**
Graduating Student,
Department of Civil Engineering,
National Technical University of Athens,
Athens, Greece 147

# Clamped Plates on Pasternak-Type Elastic Foundation by the Boundary Element Method

*A boundary element solution is developed for the analysis of thin elastic clamped plates of any shape resting on a Pasternak-type elastic foundation. The plate may have holes and it is subjected to concentrated loads, line loads, and distributed loads. The analysis is complete, i.e., deflections, stress resultants, subgrade reactions, and reactions on the boundary are evaluated. Several numerical examples are worked out and the results are compared with those available from analytical solutions. The efficiency of the BEM is demonstrated and discussed.*

## 1 Introduction

Biparametric elastic foundation models have been developed to overcome the inadequacy of Winkler's model in describing the real soil response and the mathematical complexity of the three-dimensional continuum. They are characterized by two independent elastic constants and they are derived either as an extension of the Winkler model by assuming interaction between the spring elements (Filonenko-Borodich, 1940; Hetenyi, 1946; Pasternak, 1954; Kerr, 1964) or by simplifying the three-dimensional continuum (Reissner, 1958; Vlasov and Leontiev, 1966). Among them, the Pasternak-type foundation model is the most natural extension of the Winkler model for homogeneous soil deposit and the next higher approximation to the foundation response (Kerr, 1964). Although this foundation model can adequately approximate the soil-structure interaction, the analysis of plates resting on it must overcome practically insurmountable mathematical difficulties when a general analytical solution to the governing boundary value problem is sought. Thus, only plates with simple geometry and loading have been treated analytically, such as circular plates with axisymmetric loading or rectangular plates with uniform loading. On the other hand approximate methods (Galerkin's, Ritz's) and numerical methods (finite difference, finite element) have also been used. However, the application of these methods has been restricted to simple geometries. An extensive and lucid literature on the subject at hand is found in Vlasov and Leontiev (1966) and Selvadurai (1979). Recently (Balas et al., 1984), a boundary integral equation formulation of the problem has been presented with application to a circular plate under a concentrated force at the center.

In this investigation a boundary element solution to the problem of thin elastic clamped plates resting on a Pasternak-type elastic foundation is developed. The shape of the plate is arbitrary and it may have holes while its boundary may have corners. The plate may be subjected to any kind of loading (concentrated loads, line loads, distributed loads). The analysis is complete in the sense that deflections, stress resultants, and subgrade reactions at interior points as well as reaction forces and moments on the boundary are fully evaluated. The numerical technique presented herein for the solution of the coupled boundary singular integral equations and for the computation of all the field quantities is very efficient. In case of linearly varying loading, the efficiency of the method is improved by converting the domain integrals into line integrals, thus reducing drastically the required computer time. Numerical results are obtained for circular plates, rectangular plates, and plates with a composite shape. They are compared with those obtained from existing analytical solutions. The accuracy of the results is very good, notwithstanding the complexity of the kernel functions, which, in this case, are real and imaginary parts of Hankel functions with complex argument. Finally, the solution to plates resting on a Winkler foundation as well as to plates not resting on a subgrade are obtained as special cases for appropriate values of the elastic constants.

## 2 Formulation of the Boundary Value Problem

Consider a thin elastic plate of thickness $h$, occupying the two-dimensional multiply-connected region $R$ of the plane, bounded by the $M+1$ curves $C_0$, $C_1$, $C_2$, . . . , $C_M$ and resting on a Pasternak-type elastic foundation with subgrade reaction modulus $k$ and shear modulus $G$. The curves $C_i$ ($i=0, 1, 2, \ldots M$) may be piecewise smooth, i.e., the boundary of the plate may have a finite number of corners (Fig. 1).

Assuming that the plate maintains contact with the subgrade and that there are no friction forces at the interface, its deflection $w(P)$ at any point $P \epsilon R$ satisfies the following differential equation (Kerr, 1964)

$$Lw = f(P)/D \tag{1}$$

where $f(P)$ is the transverse loading, $D$ is the flexural rigidity $[D = Eh^3/12(1-\nu^2)]$ of the plate and $L$ is an operator defined as

Contributed by the Applied Mechanics Division for publication in the JOURNAL OF APPLIED MECHANICS.

Discussion on this paper should be addressed to the Editorial Department, ASME, United Engineering Center, 345 East 47th Street, New York, N.Y. 10017, and will be accepted until two months after final publication of the paper itself in the JOURNAL OF APPLIED MECHANICS. Manuscript received by ASME Applied Mechanics Division September 9, 1985; final revision February 20, 1986.

$$L=\nabla^4-\frac{G}{D}\nabla^2+\frac{k}{D},\quad \nabla^2=\frac{\partial^2}{\partial x^2}+\frac{\partial^2}{\partial y^2},\quad \nabla^4=(\nabla^2)^2 \tag{2}$$

In this case the interaction pressure $p$ between plate and subgrade is given as

$$p=kw-G\nabla^2 w \tag{3}$$

Moreover, the deflection of the plate must satisfy the following conditions on the boundary $C=\bigcup_{i=0}^{M} C_i$ of the plate

$$w=0,\quad \frac{\partial w}{\partial n}=0 \tag{4a,b}$$

where $\partial w/\partial n$ denotes the directional derivative along the outward normal to the boundary.

The bending moments $M_n$ and $M_t$, the twisting moment $M_{nt}$, and the effective shear force $V_n$ acting on the boundary of the plate are related to the deflection $w$ by the following relations (Katsikadelis and Armenakas, 1984a).

$$M_n=-D\nabla^2 w \qquad M_t=-\nu D\nabla^2 w \tag{5a,b}$$

$$M_{nt}=0 \qquad V_n=-D\frac{\partial}{\partial n}\nabla^2 w \tag{5c,d}$$

## 3 Integral Representation of the Solution

The integral representation of the solution can be obtained by using the Green identity for the operator $L$ and the fundamental solution to equation (1).

The Green identity for the self-adjoint operator $L$ is:

$$\iint_R (vLw-wLv)d\sigma=\int_C\left[v\frac{\partial}{\partial n}\nabla^2 w-\frac{\partial v}{\partial n}\nabla^2 w\right.$$

$$\left.-w\frac{\partial}{\partial n}\nabla^2 v+\frac{\partial w}{\partial n}\nabla^2 v-\frac{G}{D}v\frac{\partial w}{\partial n}+\frac{G}{D}w\frac{\partial v}{\partial n}\right]ds \tag{6}$$

where $\partial/\partial n$ denotes the outward normal derivative.

Relation (6) is readily obtained by combining the Rayleigh-Green identity (Katsikadelis, 1982) for the biharmonic operator with the classical Green identity for the harmonic operator (equation (A7) in the Appendix). Relation (6) is valid for any two functions $w$ and $v$, which are four times continuously differentiable inside the region $R$ and three times continuously differentiable on its boundary $C$.

The fundamental solution to equation (1) is a singular particular solution of the following differential equation

$$Lv=\delta(Q-P)/D \tag{7}$$

in which $\delta(Q-P)$ is the Dirac $\delta$-function, $Q$ is the field point, and $P$ is the source point. The nature of the solution to equation (7) depends on the quantity $\mu=G^2/4kD$. In this investigation only the case $\mu<1$ is considered which seems to be valid for usual foundation materials (Kerr, 1964). For these values of $\mu$ the solution to equation (7) is given as (Vlasov and Leontiev, 1966):

$$v=v(P,Q)=v(Q,P)=\frac{\ell^2}{4D\sin 2\theta}\mathrm{Re}[H_o^{(1)}(\beta\rho)] \tag{8}$$

where

$$\ell=\sqrt[4]{D/k},\quad \rho=r/\ell \tag{9a,b}$$

$$\beta=\cos\theta+i\sin\theta,\quad 2\theta=\arctan(-\sqrt{1/\mu-1}) \tag{9c,d}$$

$r=|P\to Q|$ is the distance between the points $P$, $Q$ and $\mathrm{Re}[H_o^{(1)}(\beta\rho)]$ denotes the real part of the zero order Hankel function of the first kind. Notice that when $G$ approaches 0, it can be shown that $v(P,Q)$ reduces to $-(\ell^2/2\pi D)kei(\rho)$ which is the fundamental solution to the equation governing the plate resting on a Winkler-type elastic foundation (Katsikadelis and Armenakas, 1984a, 1984b).

From equation (8) it can be shown that

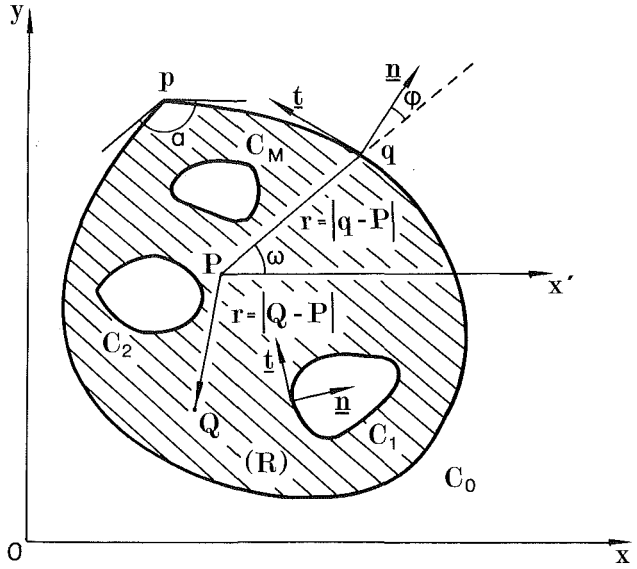


**Fig. 1 Two dimensional region *R* occupied by the plate**

$$\frac{\partial v}{\partial n}=\frac{\ell}{4D\sin 2\theta}V'(\rho)\cos\varphi \tag{10a}$$

$$\nabla^2 v=\frac{1}{4D\sin 2\theta}U(\rho) \tag{10b}$$

$$\frac{\partial}{\partial n}\nabla^2 v=\frac{1}{4\ell D\sin 2\theta}U'(\rho)\cos\varphi \tag{10c}$$

in which $(\,)'$ denotes differentiation with respect to the argument $\rho$, $\varphi$ is the angle between $\mathbf{r}$ and $\mathbf{n}$ (see Fig. 1), and

$$V(\rho)=\mathrm{Re}[H_o^{(1)}(\beta\rho)] \tag{11a}$$

$$V'(\rho)=\mathrm{Re}[-\beta H_1^{(1)}(\beta\rho)]$$
$$=-\cos\theta\,\mathrm{Re}[H_1^{(1)}(\beta\rho)]+\sin\theta\, Im[H_1^{(1)}(\beta\rho)] \tag{11b}$$

$$U(\rho)=\mathrm{Re}[-\beta^2 H_o^{(1)}(\beta\rho)]$$
$$=-\cos 2\theta\,\mathrm{Re}[H_o^{(1)}(\beta\rho)]+\sin 2\theta\, Im[H_o^{(1)}(\beta\rho)] \tag{11c}$$

$$U'(\rho)=\mathrm{Re}[\beta^3 H_1^{(1)}(\beta\rho)]$$
$$=\cos 3\theta\,\mathrm{Re}[H_1^{(1)}(\beta\rho)]-\sin 3\theta\, Im[H_1^{(1)}(\beta\rho)] \tag{11d}$$

The real valued functions $\mathrm{Re}[H_o^{(1)}(\beta\rho)]$, $Im[H_o^{(1)}(\beta\rho)]$, $\mathrm{Re}[H_1^{(1)}(\beta\rho)]$, $Im[H_1^{(1)}(\beta\rho)]$ involved in the aforegoing relations (11) are evaluated, for both small and large arguments, from their series expressions which are given in Zinke (1959).

It can be shown that for $\rho\to 0$ it is

$$\lim_{\rho\to 0} V(\rho)=1-2\theta/\pi,\qquad \lim_{\rho\to 0} V'(\rho)=0 \tag{12a,b}$$

$$\lim_{\rho\to 0} U(\rho)\sim \ell n\rho,\qquad \lim_{\rho\to 0} U'(\rho)\sim\frac{1}{\rho} \tag{12c,d}$$

$$\lim_{\rho\to 0}[\rho V'(\rho)]=0,\qquad \lim_{\rho\to 0}[\rho U'(\rho)]=2\sin 2\theta/\pi \tag{12e,f}$$

Applying equation (6) for the deflection of the plate $w$ and the fundamental solution $v$, which satisfy equations (1) and (7), respectively, using relations (8, 10$a$, 11$a$) and the boundary conditions (4$a$, $b$) the integral representation for the deflection $w(P)$ is obtained as

$$w(P)=\iint_R v(P,Q)f(Q)d\sigma_Q-D\int_C\left[v(P,q)\Psi(q)\right.$$

$$\left.-\frac{\partial v(P,q)}{\partial n_q}\Phi(q)\right]ds_q=\frac{\ell^2}{4\sin 2\theta}[F(P)-J_1(P)+J_2(P)] \tag{13}$$

where the following notation has been introduced for conciseness

$$\Phi(q)=\nabla^2 w(q), \quad \Psi(q)=\frac{\partial}{\partial n_q}\nabla^2 w(q) \tag{14a,b}$$

$$F(P)=\frac{1}{D}\iint_R V(\rho_{PQ})f(Q)d\sigma_Q \tag{15}$$

$$J_1(P)=\int_C V(\rho_{Pq})\Psi(q)ds_q,$$

$$J_2(P)=\int_C \rho_{Pq}V'(\rho_{Pq})\Phi(q)d\omega_q \tag{16a,b}$$

$$\rho_{Pq}=|P-q|/\ell, \qquad \omega=\widehat{\mathbf{x},\mathbf{r}}$$

Notice that in equation (16*b*) the relation $\cos\varphi ds = rd\omega$ has been used (Katsikadelis, 1982). In the aforegoing relations, points inside the region $R$ are denoted by uppercase letters, while points on the boundary $C$ are denoted by lowercase letters. Moreover, the subscript of the elements $d\sigma$, and $ds$ indicates the point that varies during integration. Furthermore, $\partial/\partial n_q$ denotes that the normal derivative is taken with respect to point $q$.

From relations (5) it is seen that the boundary quantities $\nabla^2 w$ and $\partial/\partial n\nabla^2 w$ appearing in the line integral of equation (13) have a direct physical meaning.

## 4 Derivation of the Boundary Integral Equations

In equation (13) the loading function $f(Q)$ is given at every point in $R$. Moreover, the function $v(P,Q)$ and its derivatives are obtained from equations (8) and (10). However, the functions $\Psi(q)$ and $\Phi(q)$ are not known at the points of the boundary $C$. These two unknown boundary quantities are established from the solution of two coupled boundary integral equations which are derived using the procedure presented in Katsikadelis and Armenakas (1984a). Thus, the first boundary integral equation is established from equation (13) by letting point $P$ approach a point $p$ on the boundary $C$. The existence of the line integrals in equation (13) for $P\equiv p\epsilon C$ and their continuity as $P\to p\epsilon C$ can be easily concluded from relations (12*a*,*b*). Consequently, taking into account that $w(p)=0$ the first boundary integral equation is obtained as

$$-\int_C \rho_{pq}V'(\rho_{pq})\Phi(q)d\omega_q+\int_C V(\rho_{pq})\Psi(q)ds_q=F(p) \tag{17}$$

The second boundary integral equation is obtained by applying the operator $\nabla^2$ on both sides of equation (13) and by letting point $P$ approach a point $p$ on the boundary. Thus

$$\nabla^2 w(p)=\iint_R \nabla^2 v(p,Q)f(Q)d\sigma_Q$$

$$-D\lim_{P\to p}\int_C \nabla^2 v(P,q)\Psi(q)ds_q$$

$$+D\lim_{P\to p}\int_C \frac{\partial}{\partial n}\nabla^2 v(P,q)\Phi(q)ds_q \tag{18}$$

By virtue of equations (10*b*,*c*) and (12*c*,*d*) it is seen that, the first line integral on the right-hand side of equation (18) represents a single layer potential due to a mass distribution $\Psi(q)$, while the second line integral represents a double layer potential due to a mass distribution $\Phi(q)$. Hence, both line integrals exist for $P\equiv p\epsilon C$. Moreover, the first line integral is continuous, while the second line integral exhibits a discontinuity jump as $P\to p\epsilon C$ (Courant and Hilbert, 1953) which is equal to

$$\lim_{P\to p}\int_C \frac{\partial}{\partial n}\nabla^2 v(P,q)\Phi(q)ds_q$$

$$-\int_C \frac{\partial}{\partial n}\nabla^2 v(p,q)\Phi(q)ds_q=\frac{2\pi-\alpha}{2\pi D}\Phi(p) \tag{19}$$

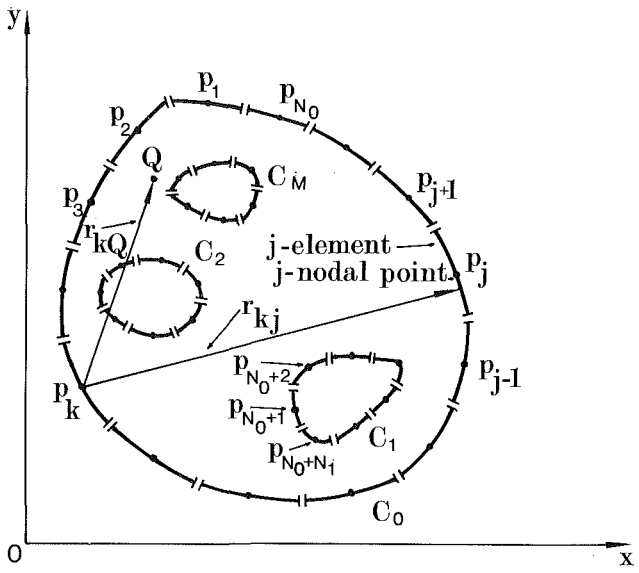


**Fig. 2 Discretization of the boundary**

where $\alpha$ is the angle between the tangents at point $p$ (see Fig. 1). It is $\alpha=\pi$ when the boundary is smooth at point $p$. Taking into account equation (19), the second boundary integral equation is obtained from equation (18) as

$$\frac{2\alpha\sin 2\theta}{\pi}\Phi(p)+\int_C U(\rho_{pq})\Psi(q)ds_q$$

$$-\int_C \rho_{pq}U'(\rho_{pq})\Phi(q)d\omega_q=G(p) \tag{20}$$

in which

$$G(p)=\frac{1}{D}\iint_R U(\rho_{pQ})f(Q)d\sigma_Q \tag{21}$$

For any given geometry of the clamped boundary of the plate, the functions $\Phi(s)$ and $\Psi(s)$ may be obtained from the solution of the coupled boundary integral equations (17) and (20). Once the functions $\Phi(s)$ and $\Psi(s)$ are known, the solution to the boundary value problem (equations (1) and (4)) may be obtained from equation (13).

## 5 Numerical Analysis

The numerical solution of the coupled boundary singular integral equations (17) and (20) is accomplished using the boundary element approach. In this approach the boundary is divided into $N$ intervals, not necessarily equal, referred to as boundary elements. The end points of each element are referred to as extreme points. Each boundary element is approximated by a given curve (straight line, parabolic arc, etc.) and the unknown boundary functions $\Phi$, $\Psi$ are approximated by a polynomial (constant, linearly varying, parabolically varying, etc.). The points on which the unknown functions are evaluated are referred to as nodal points.

In this investigation each boundary $C_i$ is divided into $N_i$ elements ($i=0, 1, \ldots, M$) not necessarily equal. The center of the elements or other points near them are taken as their nodes. The elements on the external boundary are numbered consecutively counterclockwise while on the internal boundaries clockwise (Fig. 2). The values of $\Phi$ and $\Psi$ are assumed constant on each element (step function assumption) and equal to their values at the nodal point of each element. Moreover, the curved elements are approximated by parabolic arcs (Katsikadelis and Sapountzakis, 1985). This approximation reduces appreciably the error due to the approximation of

curved boundaries by straight line elements. Denoting by $\Phi_j$ and $\Psi_j$ the values of $\Phi$ and $\Psi$ at the $j$th nodal point (i.e., the nodal point of the $j$ element), the integral equations (17) and (20) are transformed into the following system of $2N$ $\left(N=\sum_{i=0}^{M} N_i\right)$ simultaneous algebraic equations

$$\sum_{j=1}^{N} \alpha_{kj}\Phi_j + \sum_{j=1}^{N} b_{kj}\Psi_j = F_k \quad (k=1,2,\ldots,N) \tag{22a}$$

$$\sum_{j=1}^{N} \left(C_{kj}+\frac{2\alpha}{\pi}\sin 2\theta\delta_{kj}\right)\Phi_j + \sum_{j=1}^{N} d_{kj}\Psi_j = G_k \quad (k=1,2,\ldots,N) \tag{22b}$$

in which $\delta_{kj}$ is the Kronecker delta and

$$\alpha_{kj} = -\int_j \rho_{kq}V'(\rho_{kq})d\omega_q, \quad b_{kj} = \int_j V(\rho_{kq})ds_q \tag{23a,b}$$

$$c_{kj} = -\int_j \rho_{kq}U'(\rho_{kq})d\omega_q, \quad d_{kj} = \int_j U(\rho_{kq})ds_q \tag{23c,d}$$

$$F_k = \frac{1}{D}\int\int_R V(\rho_{kQ})f(Q)d\sigma_Q,$$

$$G_k = \frac{1}{D}\int\int_R U(\rho_{kQ})f(Q)d\sigma_Q \tag{23e,f}$$

$$\rho_{kq} = |p_k - q|/\ell, \quad \rho_{kQ} = |p_k - Q|/\ell, \quad Q\epsilon R, p_k\epsilon C, \quad q\epsilon j\text{-element}$$

In relations (23$a$, $b$, $c$, $d$), the symbol $\int_j$ denotes integration on the $j$-element; point $p_k$ is a nodal point.

**Evaluation of Line Integrals $\alpha_{kj}$, $\mathbf{b}_{kj}$, $\mathbf{c}_{kj}$, and $\mathbf{d}_{kj}$.** When $k\neq j$ ($\rho\neq 0$), these integrals can be evaluated using any of the known numerical techniques for the evaluation of line integrals. In this investigation the curved boundary element is approximated by a parabolic arc passing through its nodal and extreme points and its value is computed using eight-point Gaussian quadrature. When $k=j$, the argument $\rho$ vanishes for $q=p_k$. From relations (12$a$), (12$e$), and (12$f$) it is seen that the line integrals $\alpha_{kk}$, $b_{kk}$, and $c_{kk}$ are not singular and consequently they are evaluated as in the case $k\neq j$. However, as it is seen from relation (12$c$), the line integral $d_{kk}$ has a logarithmic singularity and it is evaluated using the technique presented in Katsikadelis and Armenakas (1985).

**Evaluation of Double Integrals $\mathbf{F}_k$ and $\mathbf{G}_k$.** We may distinguish the following four cases:

*a*) The plate is subjected to a concentrated load $P$ at a point $Q_o$. In this case, the loading function $f(Q)$ can be represented as

$$f(Q) = P\delta(Q-Q_o) \tag{24}$$

Using relation (24) the values of the integrals (23$e$,$f$) are

$$F_k = \frac{P}{D}V(\rho_{kQ_o}), \quad G_k = \frac{P}{D}U(\rho_{kQ_o}) \tag{25a,b}$$

where $\rho_{kQ_o} = |p_k - Q_o|/\ell$.

*b*) The plate is subjected to a line load $p(s)$ distributed along a curve $L^*$. In this case the double integrals (23$e$,$f$) are evaluated using relations (25$a$, $b$) from the following line integrals along the curve $L^*$

$$F_k = \frac{1}{D}\int_{L^*} p(Q)V(\rho_{kQ})ds_Q,$$

$$G_k = \frac{1}{D}\int_{L^*} p(Q)U(\rho_{kQ})ds_Q \tag{26a,b}$$

where $\rho_{kQ} = |p_k - Q|/\ell$, $Q\epsilon L^*$.

*c*) The plate is subjected to a uniform or a linearly varying load distributed over an area $R^*\subseteq R$ of the plate bounded by a curve $C^*$. In this case, it is $\nabla^2 f = 0$ and by virtue of relations ($A6$), ($A7$), ($A8$), and ($A9$) in the Appendix the double integrals (23$e$, $f$) can be converted into the following line integrals on the curve $C^*$.

$$F_k = -\cos 2\theta G_k - \frac{\ell^2\sin 2\theta}{D}\left[\epsilon f(p_k) + \int_{C^*}\rho_{kq}I'(\rho_{kq})f(q)d\omega_q - \int_{C^*} I(\rho_{kq})\frac{\partial f(q)}{\partial n_q}ds_q\right] \tag{27a}$$

$$G_k = \frac{\ell^2}{D}\left[\int_{C^*}\rho_{kq}V'(\rho_{kq})f(q)d\omega_q - \int_{C^*} V(\rho_{kq})\frac{\partial f(q)}{\partial n_q}ds_q\right] \tag{27b}$$

where $\rho_{kq} = |p_k - q|/\ell$, $q\epsilon C^*$; $I(\rho) = Im[H_o^{(1)}(\beta\rho)]$; $\epsilon$ is given in the Appendix.

The substitution of the domain integrals by line integrals reduces drastically the required computer time. The line integrals (27$a$, $b$) as well as (26$a$, $b$) are evaluated numerically employing the technique presented in Katsikadelis and Armenakas (1985). Thus, the curve $C^*$, $L^*$, respectively, is approximated by a finite number of parabolic elements. On each element the line integral is computed and the resulting partial values are summed.

*d*) In the general case where $f(Q)$ is an arbitrary function, the domain integrals (23$e$, $f$) are evaluated using the method presented in Katsikadelis and Armenakas (1983).

## 6 Evaluation of the Deflections, Stress Resultants and Subgrade Reactions

When the integrals $\alpha_{kj}$, $b_{kj}$, $c_{kj}$, $d_{kj}$, $F_k$, and $G_k$ are established, the system of simultaneous algebraic equations (22$a$, $b$) is solved and the values $\Phi_j$ and $\Psi_j$ of the functions $\Phi(s)$ and $\Psi(s)$ at the nodal points are obtained. These values can be used to obtain the deflection $w(P)$ and the stress resultants at any point $P$ in the interior of the plate.

The deflections $w(P)$ is obtained from its integral representation (13). The line integrals $J_1(P)$ and $J_2(P)$ are computed from the relations

$$J_1(P) = \sum_{j=1}^{N}\Psi_j\int_j V(\rho_{Pq})ds_q,$$

$$J_2(P) = \sum_{j=1}^{N}\Phi_j\int_j \rho_{Pq}V'(\rho_{Pq})d\omega_q \tag{28a,b}$$

For the computation of the double integral $F(P)$ in relation (15) we distinguish again four cases as for the integral $F_k$ in the previous section.

Referring to relations (5) and (14) it is apparent that the bending moments $M_n$, $M_t$ and the reaction force $V_n$ on the boundary of the plate are readily computed from the values of $\Phi$ and $\Psi$.

The bending moments $M_x$, $M_y$, the twisting moment $M_{xy}$ and the shear forces $Q_x$ and $Q_y$ at any point of the plate are equal to

$$M_x = -D\left(\frac{\partial^2 w}{\partial x^2} + \nu\frac{\partial^2 w}{\partial y^2}\right), \quad Q_x = -D\frac{\partial}{\partial x}\nabla^2 w \tag{29a,b}$$

$$M_y = -D\left(\frac{\partial^2 w}{\partial y^2} + \nu\frac{\partial^2 w}{\partial x^2}\right), \quad Q_y = -D\frac{\partial}{\partial y}\nabla^2 w \tag{29c,d}$$

$$M_{xy} = -M_{yx} = D(1-\nu)\frac{\partial^2 w}{\partial x\partial y} \tag{29e}$$

The second and third order derivatives of the deflections in

equation (29) may be evaluated from the computed values of the deflections with sufficient accuracy using numerical differentiation. However, the accuracy is increased and the computer time is considerably reduced when they are evaluated by direct differentiation of relation (13) using the following combinations of derivatives.

$$d_i = \frac{1}{4\sin 2\theta}\left[\frac{1}{D}\int\int_R K_i(\rho) f d\sigma - \int_C K_i(\rho)\Psi ds + \frac{1}{\ell}\int_C \Lambda_i(\rho)\Phi ds\right] \quad (i=1,2,3,4,5) \tag{30}$$

where

$$d_1 = \frac{\partial^2 w}{\partial x^2} + \frac{\partial^2 w}{\partial y^2},\quad d_2 = \frac{\partial^2 w}{\partial x^2} - \frac{\partial^2 w}{\partial y^2},\quad d_3 = 2\frac{\partial^2 w}{\partial x \partial y}, \tag{31a,b,c}$$

$$d_4 = -\ell\frac{\partial}{\partial x}\nabla^2 w,\quad d_5 = -\ell\frac{\partial}{\partial y}\nabla^2 w \tag{31d,e}$$

$$K_1(\rho) = U(\rho),\quad K_2(\rho) = C(\rho)\cos 2\omega,\quad K_3(\rho) = C(\rho)\sin 2\omega \tag{32a,b,c}$$

$$K_4(\rho) = U'(\rho)\cos\omega,\quad K_5(\rho) = U'(\rho)\sin\omega \tag{32d,e}$$

$$\Lambda_1(\rho) = U'(\rho)\cos\varphi,$$

$$\Lambda_2(\rho) = U'(\rho)\cos\varphi\cos 2\omega - \frac{2}{\rho}C(\rho)\cos(2\omega-\varphi) \tag{32f,g}$$

$$\Lambda_3(\rho) = U'(\rho)\cos\varphi\sin 2\omega - \frac{2}{\rho}C(\rho)\sin(2\omega-\varphi) \tag{32h}$$

$$\Lambda_4(\rho) = -\left[\frac{1}{\rho}U'(\rho)\cos(\omega-\varphi) + V(\rho)\cos\omega\cos\varphi + 2U(\rho)\cos 2\theta\cos\omega\cos\varphi\right] \tag{32i}$$

$$\Lambda_5(\rho) = -\left[\frac{1}{\rho}U'(\rho)\sin(\omega-\varphi) + V(\rho)\sin\omega\cos\varphi + 2U(\rho)\cos 2\theta\sin\omega\cos\varphi\right] \tag{32j}$$

$$C(\rho) = U(\rho) - \frac{2}{\rho}V'(\rho) \tag{32k}$$

For an arbitrary loading function $f(Q)$ the double integrals in equation (30) may be evaluated using the technique presented in Katsikadelis and Armenakas (1983).

When the loading is due to a concentrated force $P$ at some point $Q$ the double integrals in relation (30) can be directly evaluated from relations analogous to (25). Moreover, when the loading is due to a line load along a curve $L^*$, the double integrals in relation (30) are reduced to line integrals on the curve $L^*$ and they are computed from relations analogous to (26). Finally, when the plate is loaded by a uniform or a linearly varying load distributed over a region $R^* \subseteq R$ bounded by a curve $C^*$ the double integrals in relation (30) can be converted into line integrals. Thus, using integration by parts and employing relations (A6) and (A8) in Appendix, we obtain

$$\int\int_{R^*} f\left(\frac{\partial^2}{\partial x^2} - \frac{\partial^2}{\partial y^2}\right)V(\rho)d\sigma = \frac{1}{\ell}\int_{C^*} fV'(\rho)\cos(2\omega+\varphi)ds - \int_{C^*}\left[\frac{\partial f}{\partial \xi}\cos(\omega+\varphi) - \frac{\partial f}{\partial \eta}\sin(\omega+\varphi)\right]V(\rho)ds \tag{33a}$$

$$\int\int_{R^*} f\frac{\partial^2}{\partial x \partial y}V(\rho)d\sigma = \frac{1}{\ell}\int_{C^*} fV'(\rho)\sin\omega\cos(\omega+\varphi)ds - \int_{C^*}\frac{\partial f}{\partial \xi}V(\rho)\sin(\omega+\varphi)ds \tag{33b}$$

$$\int\int_{R^*} f\frac{\partial}{\partial x}\nabla^2 V(\rho)d\sigma = -\frac{1}{\ell^2}\int_{C^*} fU(\rho)\cos(\omega+\varphi)ds + \frac{1}{\ell}\int_{C^*}\frac{\partial f}{\partial \xi}V'(\rho)\cos\varphi ds \tag{33c}$$

$$\int\int_{R^*} f\frac{\partial}{\partial y}\nabla^2 V(\rho)d\sigma = -\frac{1}{\ell^2}\int_{C^*} fU(\rho)\sin(\omega+\varphi)ds + \frac{1}{\ell}\int_{C^*}\frac{\partial f}{\partial n}V'(\rho)\cos\varphi ds \tag{33d}$$

where $x, y \epsilon R$ and $\xi, \eta \epsilon C^*$.

**Table 1 Percent error in the deflection $w$, bending moment $M_r$, and reaction force $V_n$ in a clamped circular plate with radius $a$, resting on an elastic foundation ($\lambda = 10$, $s = 13$), and subjected to a uniform load $q$**

| Number of BE | Error in $w$ $r = .5a$ | Error in $M_r$ $r = .5a$ | Error in $V_n$ $r = a$ |
|---|---|---|---|
| 10 | .051 | 1.056 | .836 |
| 20 | .006 | .137 | .117 |
| 30 | .002 | .041 | .036 |
| 40 | .001 | .017 | .015 |
| 50 | .000 | .009 | .008 |
| 60 | .000 | .005 | .005 |
| 70 | .000 | .003 | .003 |
| 80 | .000 | .002 | .002 |

## 7 Numerical Results

A computer program has been written for the numerical evaluation of the response of clamped plates resting on a Pasternak-type elastic foundation by integrating the boundary integral equations (17) and (20) using the numerical technique described in Section 5. Numerical results have been obtained for circular plates with or without holes, rectangular plates and a plate of composite shape subjected to concentrated loads, uniform, and linearly varying loads. The obtained results are in excellent agreement with those obtained from analytical solutions or other numerical solutions. When $G \to 0$ the solution for the plate resting on a Winkler-type elastic foundation is obtained, while when both constants, $G$ and $k$, are small, the solution for the plate not resting on an elastic subgrade is obtained.

For the presentation of the numerical results the following dimensionless parameters are introduced which are established by writing equation (1) in a dimensionless form

$$s = a/\sqrt{D/G},\quad \lambda = a/\sqrt[4]{D/k}$$

where $a$ is a characteristic length of the plate (e.g., the radius of a circular plate, the length of one side of a rectangular plate, etc.). The shear modulus $G$ may vary between 0 to 40MN/m, while the subgrade reaction modulus $k$ may vary from 0 to 200MN/m$^3$. Thus, for usual engineering applications it is $0 \le s \le 30$ and $0 \le \lambda \le 20$. In computations, it may be set $s = 0$. However, the value $\lambda = 0$ must be excluded because it raises computational difficulties. A small value of $\lambda$ (say $\lambda = 0.1$ to 0.5) and $s = 0$ give accurate results for the plate not resting on subgrade.

In Table 1, the percent error in the numerical results obtain-

**Table 2 Deflections $\bar{w} = w/(Pa^2/D)$ in a clamped circular plate with radius $a$ subjected to a concentrated force $P$ at its center**

| | $\lambda = .134$, $s = 0$ | | $\lambda = 12$, $s = 0$ | | $\lambda = 12$, $s = 15$ | |
|---|---|---|---|---|---|---|
| $r/a$ | analytic | BEM | analytic | BEM | analytic | BEM |
| 0 | .19894E−01 | .19894E−01 | .86806E−03 | .86806E−03 | .59681E−03 | .59681E−03 |
| 0.2 | .16537E−01 | .16537E−01 | .13953E−03 | .13953E−03 | .11590E−03 | .11590E−03 |
| 0.4 | .10878E−01 | .10877E−01 | −.12264E−04 | −.12264E−04 | .10507E−04 | .10507E−04 |
| 0.6 | .54154E−02 | .54150E−02 | −.22695E−05 | −.22695E−05 | .51292E−06 | .51292E−06 |
| 0.8 | .14797E−02 | .14795E−02 | .35712E−06 | .35711E−06 | −.12968E−07 | −.12965E−07 |

**Table 3 Deflections, bending moments and shearing forces in a clamped circular ring-shaped plate with an inner radius $b$ and an outer radius $a = 3b$ subjected to a uniform load $q$**

| | $\lambda = .134$, $s = 0$ | | $\lambda = 12$, $s = 0$ | | $\lambda = 12$, $s = 15$ | |
|---|---|---|---|---|---|---|
| $r/b$ | analytic | BEM | analytic | BEM | analytic | BEM |
| | | | Deflections $\bar{w} = w/(qa^4/D)$ | | | |
| 1.4 | .21740E−01 | .21741E−01 | .54455E−04 | .54455E−04 | .51193E−04 | .51188E−04 |
| 1.8 | .44073E−01 | .44073E−01 | .52551E−04 | .52551E−04 | .52615E−04 | .52615E−04 |
| 2.1 | .40622E−01 | .40622E−01 | .52518E−04 | .52518E−04 | .52617E−04 | .52617E−04 |
| 2.6 | .16895E−01 | .16894E−01 | .54912E−04 | .54912E−04 | .50906E−04 | .50906E−04 |
| | | | Bending moment $\bar{M}_r = M_r/qa^2$ | | | |
| 1.0 | −.44861E+00 | −.44861E+00 | −.73420E−02 | −.73420E−02 | −.74249E−02 | −.74715E−02 |
| 1.4 | .80839E−02 | .80860E−02 | .14935E−03 | .14935E−03 | .19618E−03 | .19677E−03 |
| 1.8 | .15789E+00 | .15789E+00 | −.24074E−05 | −.24073E−05 | .55076E−06 | .55478E−06 |
| 2.2 | .13134E+00 | .13134E+00 | −.35616E−05 | −.35623E−05 | .81261E−06 | .81279E−06 |
| 2.6 | −.24062E−01 | −.24065E−01 | .17698E−03 | .17701E−03 | .22293E−03 | .22296E−03 |
| 3.0 | −.28612E+00 | −.28612E+00 | −.68067E−02 | −.68074E−02 | −.67599E−02 | −.67623E−02 |
| | | | Shearing force $\bar{Q}_r = Q_r/qa$ | | | |
| 1.0 | .14684E+01 | .14685E+01 | .12489E+00 | .12489E+00 | .16905E+00 | .16960E+00 |
| 1.4 | .70599E+00 | .70598E+00 | −.34146E−02 | −.34146E−02 | −.19353E−02 | −.19402E−02 |
| 1.8 | .19355E+00 | .19354E+00 | .95462E−04 | .95463E−04 | −.14228E−04 | −.14296E−04 |
| 2.2 | −.20528E+00 | −.20528E+00 | −.13524E−03 | −.13525E−03 | .20057E−04 | .20061E−04 |
| 2.6 | −.54293E+00 | −.54293E+00 | .40313E−02 | .40316E−02 | .22448E−02 | .22451E−02 |
| 3.0 | −.84387E+00 | −.84387E+00 | −.11555E+00 | −.11556E+00 | −.15316E+00 | −.15318E+00 |

**Table 4 Deflection $\bar{w} = w/(qa^4/D)$ and bending moments $\bar{M}_x = M_x/qa^2$ $\bar{M}_y = M_y/qa^2$ in a clamped rectangular $(a \times b)$ plate subjected to a hydrostatic load $f = qx/a$, $0 \le x \le a$, $0 \le y \le b$, for various side ratios $b/a$ ($[\lambda = 0.134$, $s = 0$, $\nu = 0.3)$. The analytical results are obtained from Timoshenko and Woinowsky-Krieger (1959)**

| | $b/a = 0.5$ | | $b/a = 1.0$ | | $b/a = 1.5$ | |
|---|---|---|---|---|---|---|
| | analytic | BEM | analytic | BEM | analytic | BEM |
| $w(a/2,b/2)$ | .080E−03 | .079E−03 | .630E−03 | .630E−03 | .110E−02 | .109E−02 |
| $M_x(a/2,b/2)$ | .198E−02 | .198E−02 | .115E−01 | .114E−01 | .184E−01 | .183E−01 |
| $M_y(a/2,b/2)$ | .515E−02 | .513E−02 | .115E−01 | .114E−01 | .102E−01 | .101E−01 |
| $M_x(a,b/2)$ | −.115E−01 | −.115E−01 | −.334E−01 | −.336E−01 | −.462E−01 | −.463E−01 |
| $M_x(0,b/2)$ | −.028E−02 | −.028E−01 | −.179E−01 | −.179E−01 | −.295E−01 | −.295E−01 |
| $M_y(a/2,b)$ | −.104E−01 | −.104E−01 | −.257E−01 | −.257E−01 | −.285E−01 | −.286E−01 |

**Table 5 Influence coefficients for a clamped rectangular $(2a \times 2b)$ plate with side ratio $b/a = 1.2$ resting on an elastic foundation with $\lambda = 5$, $s = 7$**

| Load position | Influence coefficients for $\bar{w} = w/(Pa^2/D)$ at $x = 0$, $y = 0$ | | | | |
|---|---|---|---|---|---|
| $x/a$ | | | | | |
| $y/b$ | 0 | 0.2 | 0.4 | 0.6 | 0.8 |
| 0.8 | .5162E−04 | .4602E−04 | .3248E−04 | .1727E−04 | .5126E−05 |
| 0.6 | .2121E−03 | .1858E−03 | .1261E−03 | .6504E−04 | .1970E−04 |
| 0.4 | .6331E−03 | .5314E−03 | .3287E−03 | .1558E−03 | .4547E−04 |
| 0.2 | .1664E−02 | .1261E−02 | .6620E−03 | .2796E−03 | .7735E−04 |
| 0 | .3197E−02 | .1920E−02 | .8765E−03 | .3465E−03 | .9330E−04 |
| | Influence coefficients for $\bar{M}_x = M_x/P$ at $x = 0$, $y = 0$ ($\nu = 0.3$) | | | | |
| $x/a$ | | | | | |
| $y/b$ | 0 | 0.2 | 0.4 | 0.6 | 0.8 |
| 0.8 | −.2970E−04 | −.6935E−04 | −.1236E−03 | −.1099E−03 | −.4193E−04 |
| 0.6 | .1802E−03 | −.1224E−03 | −.5151E−03 | −.4878E−03 | −.1915E−03 |
| 0.4 | .2578E−02 | .3950E−03 | −.1750E−02 | −.1565E−02 | −.5783E−03 |
| 0.2 | .2081E−01 | .2087E−02 | −.5684E−02 | −.3793E−02 | −.1241E−02 |
| 0 | .1000E+31 | −.4089E−02 | −.1025E−01 | −.5392E−02 | −.1641E−02 |

ed using the BEM as compared with those obtained from analytical solutions (Selvadurai, 1979) is presented versus the number of boundary elements for a clamped circular plate resting on an elastic foundation ($\lambda = 10$ and $s = 13$), subjected to a uniform load. It is apparent that only a few boundary elements (20 to 30) are sufficient to obtain accurate results.

To demonstrate the accuracy of the BEM three more examples are worked out for which results from analytical solutions are available. Thus, in Table 2 the deflections along the radius of a clamped circular plate subjected to a concentrated load $P$ at its center are tabulated. They are obtained on the basis of analytical solutions and also using the BEM with 32 elements. Three characteristic cases are considered: (*a*) plate not resting on an elastic foundation ($\lambda = 0.134$, $s = 0$); (*b*) plate resting on a Winkler-type foundation ($\lambda = 12$, $s = 0$); (*c*) plate resting on a Pasternak-type foundation ($\lambda = 12$, $s = 15$). The analytical solutions are obtained from Timoshenko and Woinowsky-Krieger (1959), Schleicher (1926), and Selvadurai (1979), respectively.

Moreover, in Table 3 the deflection, the bending moment and the shearing force along the radius of a clamped circular ring-shaped plate with an inner radius $b$ and an outer radius $a = 3b$ are presented when it is subjected to a uniform load $q$. The numerical results are obtained using the BEM with 32 boundary elements on each boundary and they are compared with those obtained from the analytical solutions (as in Table 2). Furthermore, in Table 4 the deflection and bending moments in a clamped rectangular plate ($a \times b$) not resting on an elastic foundation ($\lambda = 0.134$, $s = 0$) and subjected to a hydrostatic load are presented. The results are obtained using 44 boundary elements and they are compared with existing results from the analytical solution (Timoshenko and Woinowsky-Krieger, 1959).

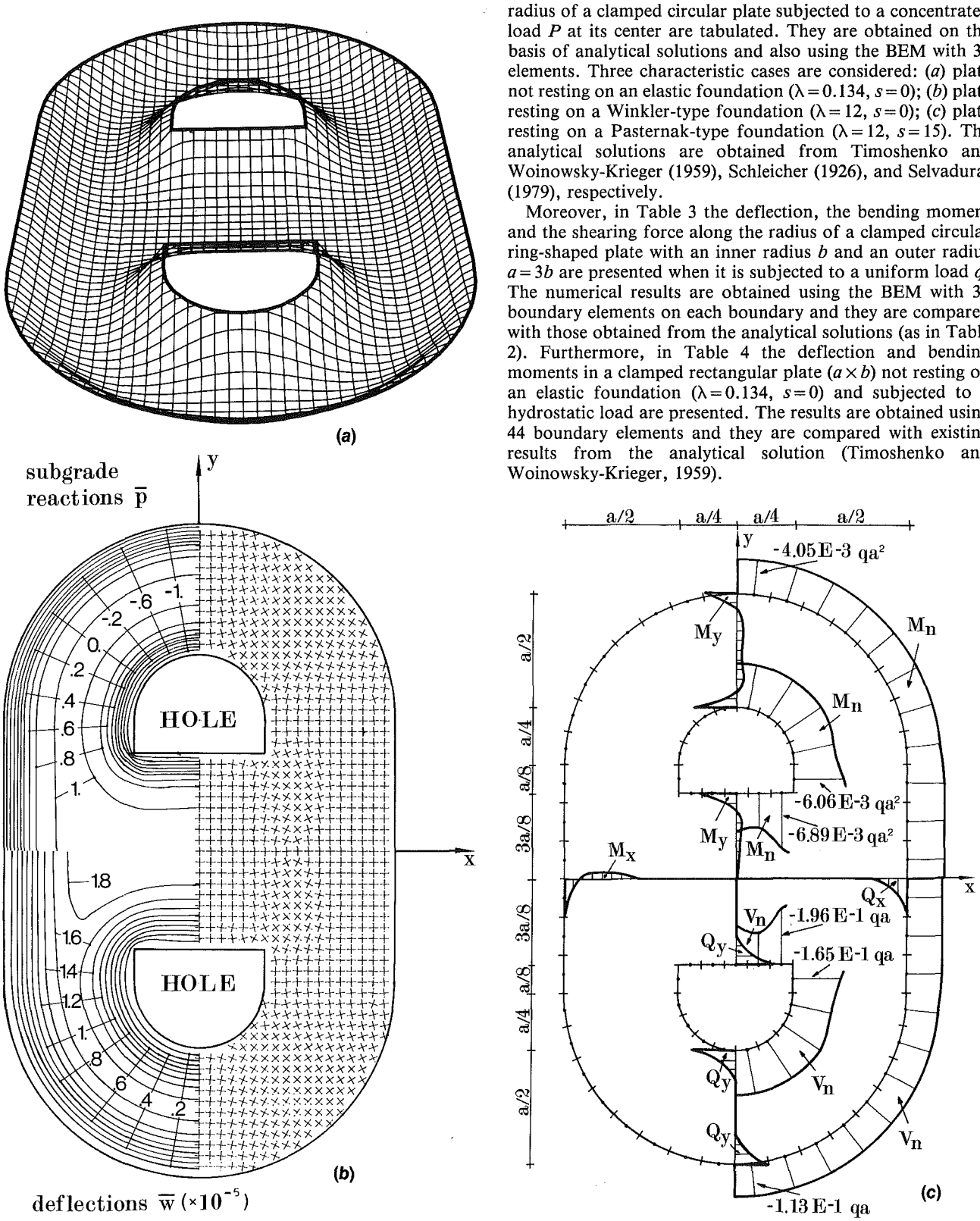


**Fig. 3 Uniformly loaded clamped plate of composite geometry resting on a Pasternak-type elastic foundation ($\lambda = 15$, $s = 18$): (*a*) Perspective of the deflection surface of the plate; (*b*) deflections $\bar{w} = w/(qa^4/D)$, subgrade reactions $\bar{p} = p/q$ and directions of principal bending moments; (*c*) boundary reactions and stress resultants**

In Table 5, the influence coefficients for the deflection $\bar{w}=w/(Pa^2/D)$ and for the bending moment $\bar{M}_x=M_x/P$ at point $x=y=0$ of a clamped rectangular plate $(2a\times 2b)$ with side ratio $b/a=1.2$ for various positions of the concentrated load $P$ are presented ($\lambda=5$, $s=7$). The obtained values differ considerably from the corresponding values for a Winkler-type foundation (see Katsikadelis and Armenakas, 1984a).

Finally, in Fig. 3 results obtained on the basis of BEM using 74 boundary elements for a clamped plate of composite shape resting on elastic foundation ($\lambda=15$, $s=18$) and subjected to a uniform load $q$ are shown. These results are considered accurate because they differ negligibly from those obtained using twice as many boundary elements.

## Conclusions

The following conclusions can be deduced from this investigation:

(*a*) The BEM solution to the problem of bending of thin plates on a biparametric elastic foundation developed herein is well suited for computer-aided analysis.

(*b*) Plates having a composite shape including holes and subjected to any kind of loading are efficiently and completely analyzed; i.e., their deflections, bending, and twisting moments, shearing forces, boundary reactions and subgrade reactions can be established with good accuracy.

(*c*) The conversion of the domain integrals into line integrals reduces drastically the computer time and renders BEM a powerful tool for analyzing difficult plate problems.

(*d*) For plates with relatively smooth boundary the constant element yields good results. The results are considerably improved if curved boundaries are approximated by parabolic arcs.

(*e*) The evaluation of the kernel functions, which are real and imaginary parts of Hankel functions with complex argument, are accurately computed from real valued series expressions.

## References


Abramowitz, M., and Stegun, I., eds., 1972, *Handbook of Mathematical Functions*, 10th Ed., Dover, New York.

Balas, J., Sladek, V., and Sladek, J., 1984, "The Boundary Integral Equation Method for Plates Resting on a Two Parameter Foundation," *Zeitschrift für Angewandte Mathematik und Mechanik*, Vol. 51, pp. 574–580.

Courant, R., and Hilbert, D., 1953, *Methods of Mathematical Physics*, Vol. 11, Interscience, New York, Chapt. IV.

Filonenko-Borodich, M. M., 1940, "Some Approximate Theories of the Elastic Foundation," in Russian, *Uchenyie Zapiski Moskovskogo Gosudarstvennogo Universiteta, Mekhanica* (Scientific Notes of the Moscow State University, Mechanics), No. 46, pp. 3–18.

Hetenyi, M., 1946, *Beams on Elastic Foundations*, The University of Michigan Press, Ann Arbor, Mich.

Katsikadelis, J. T., 1982, "The Analysis of Plates on Elastic Foundation by the Boundary Integral Equation Method," Ph.D. Dissertation, Polytechnic Institute of New York.

Katsikadelis, J. T., and Armenakas, A. E., 1983, "Numerical Evaluation of Double Integrals with a Logarithmic or a Cauchy-Type Singularity," ASME Journal of Applied Mechanics, Vol. 50, pp. 682–684.

Katsikadelis, J. T., and Armenakas, A. E., 1984a, "Analysis of Clamped Plates on Elastic Foundation by the Boundary Integral Equation Method," ASME Journal of Applied Mechanics, Vol. 51, pp. 574–580.

Katsikadelis, J. T., and Armenakas, A. E., 1984b, "Plates on Elastic Foundation by BIE Method," *Journal of Engineering Mechanics*, ASCE, Vol. 110, No. 7, pp. 1086–1105.

Katsikadelis, J. T., and Armenakas, A. E., 1985, "Numerical Evaluation of Line Integrals with a Logarithmic Singularity," *AIAA Journal*, Vol. 23, pp. 1135–1137.

Katsikadelis, J. T., and Sapountzakis, E. J., 1985, "Torsion of Composite Bars by the Boundary Element Method," *Journal of Engineering Mechanics*, ASCE, Vol. 111, No. 9, pp. 1197–1210.

Kerr, A. D., 1964, "Elastic and Viscoelastic Foundation Models," ASME Journal of Applied Mechanics, Vol. 31, pp. 491–498.

Pasternak, P. L., 1954, "On a New Method of Analysis of an Elastic Foundation by Means of two Foundation Constants," in Russian, *Gosudarstvennoe Izdatelstvo Literaturi po Stroitelstvu i Arkhitekture*, (State Publications on Construction Literature, Architecture), Moscow, USSR.

Reissner, E., 1958, "A Note on Deflection of Plates on Viscoelastic Foundation," ASME Journal of Applied Mechanics, Vol. 80, pp. 144–145.

Schleicher, F., 1926, *Kreisplatten auf Elastischer Unterlage*, Springer Verlag, Berlin.

Selvadurai, A. P. S., 1979, *Elastic Analysis of Soil-Foundation Interaction*, Elsevier, Amsterdam-Oxford-New York, Chapt. 2, pp. 27–30, Chapt. 6, pp. 223–244 and pp. 307–313.

Timoshenko, S., and Woinowsky-Krieger, S., 1959, *Theory of Plates and Shells*, 2nd Ed., McGraw-Hill, New York.

Vlasov, V. Z., and Leontiev, N. N., 1966, *Beams, Plates and Shells on Elastic Foundations*, Israel Program for Scientific Translations, Jerusalem, Chapt. IV, pp. 161–183.

Zinke, O., 1959, *Elementare Einführung in die Bessel-, Neumman- und Hankel-Functionen*, S. Hirzel Verlag, Stuttgart, pp. 31–33.


## APPENDIX

In this Appendix certain formulae are derived which are used to convert the double integrals (23*e*, *f*) and (33*a*, *b*, *c*, *d*) into line integrals when the loading function $f(Q)$ varies linearly over a region $R^*\subseteq R$ bounded by a curve $C^*$.

Consider the differential equation

$$\frac{d^2w}{dz^2}+\frac{1}{z}\frac{dw}{dz}+w=0 \tag{A1}$$

When $z=\beta\rho$, with $\rho=|P-Q|/\ell$ and $\beta=e^{i\theta}$ a complex-constant, equation (*A*1) reduces to

$$\frac{d^2w}{d\rho^2}+\frac{1}{\rho}\frac{dw}{d\rho}+\beta^2w=0 \tag{A2}$$

Equation (*A*2) is satisfied by the Hankel function (Abramowitz and Stegun, 1972)

$$H_o^{(1)}(\beta\rho)=V(\rho)+iI(\rho) \tag{A3}$$

where $V(\rho)$ and $I(\rho)$ are, respectively, the real and imaginary part of $H_o^{(1)}(\beta\rho)$.

Substituting equation (*A*3) into equation (*A*2) and separating real and imaginary parts, the following two simultaneous differential equations are obtained

$$\nabla^2V(\rho)=\sin2\theta I(\rho)-\cos2\theta V(\rho) \tag{A4}$$

$$\nabla^2I(\rho)=-\cos2\theta I(\rho)-\sin2\theta V(\rho) \tag{A5}$$

where $$\nabla^2=\frac{d^2}{d\rho^2}+\frac{1}{\rho}\frac{d}{d\rho}.$$

Elimination of $I(\rho)$ from equations (*A*4) and (*A*5) yields

$$V(\rho)=-\cos2\theta\nabla^2V(\rho)-\sin2\theta\nabla^2I(\rho) \tag{A6}$$

For any two functions $w$ and $v$ which are two times continuously differentiable in the region $R^*$ and one time continuously differentiable on its boundary $C^*$ it is valid

$$\iint_{R^*}(v\nabla^2w-w\nabla^2v)d\sigma=\int_{C^*}\left(v\frac{\partial w}{\partial n}-w\frac{\partial v}{\partial n}\right)ds \tag{A7}$$

Applying the Green identity (*A*7) for the pair of functions $v=f$, $w=V(\rho)$ and noting that $\nabla^2f=0$ we obtain

$$\iint_{R^*}\nabla^2V(\rho)f(Q)d\sigma_Q$$

$$=\ell^2\int_{C^*}\left[\frac{\partial V(\rho)}{\partial n_q}f(q)-V(\rho)\frac{\partial f(q)}{\partial n_q}\right]ds_q \tag{A8}$$

Similarly, applying the same identity for the pair of functions $v=f$ and $w=I(\rho)$ we obtain

$$\iint_{R^*}\nabla^2I(\rho)f(Q)d\sigma_Q$$

$$=\ell^2\left\{\epsilon f(P)+\int_{C^*}\left[f(q)\frac{\partial I(\rho)}{\partial n_q}-I(\rho)\frac{\partial f(q)}{\partial n_q}\right]ds_q\right\} \tag{A9}$$

where in double integrals it is $\rho=|P-Q|/\ell$, $Q\epsilon R^*$ while in line integrals, it is $\rho=|P-q|/\ell$, $q\epsilon C^*$.

The additional term $\epsilon f(P)$ in equation (A9) is due to the fact that the line integral behaves like a double layer potential. The value of the constant is established by a limiting process. Thus, isolating point $P$ by a small circle centered at point $P$, when $P$ is inside $R^*$, or by a small circular sector when point $P$ is on $C^*$, applying Green's identity (A7), letting the radius of the small circle or of the circular sector, respectively, shrink to a point and taking into account that for small values of the argument $\rho$ it is

$$\frac{\partial I(\rho)}{\partial n}=\frac{1}{\ell}I'(\rho)\cos\varphi=-\frac{1}{\ell}\{\sin\theta\mathrm{Re}[H_1^{(1)}(\beta\rho)]+\cos\theta Im[H_1^{(1)}(\beta\rho)]\}\cos\varphi\simeq-\frac{1}{\ell}\frac{2}{\pi\rho}\cos\varphi$$

we obtain

$$\epsilon=-4 \qquad \text{when } P \text{ is inside } R^* \qquad (A10a)$$

$$\epsilon=-2(2-\alpha/\pi) \qquad \text{when } P \text{ is on } C^* \qquad (A10b)$$

Note that

$$\epsilon=0 \qquad \text{when } P \text{ is outside } R^* \qquad (A10c)$$

$\alpha$ is the angle between the tangents at point $p$ of the boundary. For smooth boundaries it is $\alpha=\pi$.